Drug Delivery

DOI: 10.1002/ange.201308920

DNA-Hybrid-Gated Multifunctional Mesoporous Silica Nanocarriers for Dual-Targeted and MicroRNA-Responsive Controlled Drug Delivery**

Penghui Zhang, Fangfang Cheng, Ri Zhou, Juntao Cao, Jingjing Li, Clemens Burda, Qianhao Min, and Jun-Jie Zhu**

Abstract: *The design of an ideal drug delivery system with targeted recognition and zero premature release, especially controlled and specific release that is triggered by an exclusive endogenous stimulus, is a great challenge. A traceable and aptamer-targeted drug nanocarrier has now been developed; the nanocarrier was obtained by capping mesoporous silica-coated quantum dots with a programmable DNA hybrid, and the drug release was controlled by microRNA. Once the nanocarriers had been delivered into HeLa cells by aptamer-mediated recognition and endocytosis, the overexpressed endogenous miR-21 served as an exclusive key to unlock the nanocarriers by competitive hybridization with the DNA hybrid, which led to a sustained lethality of the HeLa cells. If microRNA that is exclusively expressed in specific pathological cell was screened, a combination of chemotherapy and gene therapy should pave the way for a targeted and personalized treatment of human diseases.*

Mesoporous silica nanoparticles (MSNPs) have been considered as the most promising candidate for the fabrication of drug delivery systems with zero premature release, targeted delivery, and spatio-temporal controlled release by virtue of their controllable mesoporous structure, a high specific surface area, and good biocompatibility.[1] More importantly, multifunctional MSNPs with targeting and tracking capabilities can be developed because mesoporous silica not only provides a modifiable interface for conjugation with recognizing biomolecules, but it also acts as a universal scaffold for combination with magnetic or luminescent materials.[2] To date, a large number of drug delivery systems that are based on MSNPs have been developed by employing nanoparticles,[3] supramolecular assemblies,[4] polymer multilayers,[5] DNA,[6] and proteins[7] as gatekeepers, and subsequently using redox chemistry,[8] changes in pH value[9] or temperature,[10] enzymes,[11] competitive binding,[6a] or photoirradiation[12] as stimuli to trigger on-command drug release. Although some capping–releasing systems are well-designed, there is still a long way to go to practically apply them in vitro and in vivo owing to the unobvious difference between tumor cells and peripheral normal tissues in terms of temperature, pH value, chemical composition, and enzyme concentration.[13] Therefore, there is an urgent need for effective drug release systems that respond to specific endogenous stimuli, in particular to biomolecules that are aberrantly expressed in tumor tissues.

MicroRNAs (miRNAs) are short non-coding RNA molecules that regulate gene expression in various cellular processes. Particularly during cancer initiation, development, and metastasis, tumors demonstrate distinct miRNA expression profiles compared to their normal tissue counterparts, thus providing novel biomarkers for cancer diagnosis[14] and classification[15] as well as potential therapeutic targets. As one of the oncogenic miRNAs, miR-21 was reported to be overexpressed in various human cancers, and inhibition of its expression by delivering antisense oligonucleotides (anti-miR-21) could activate caspase-dependent apoptosis, which would ultimately lead to the eradication of the tumor cells.[16] Furthermore, through general molecular design, the anti-miR-21 strand can be coupled with a DNA aptamer to form a DNA hybrid with a specific recognition capability towards the receptors that are overexpressed on the surfaces of the target tumor cells and with an exclusive response to miR-21 through complementary base pairing. More excitingly, because of the secondary structure of the aptamer, which may be duplex, quadruplex, or hairpin stem, the designed DNA hybrid is not only a promising target agent for dual recognition towards biomolecules and cells, but also a desirable gatekeeper for controlled drug release.

Herein, we report a proof of concept for the fabrication of a traceable and dual-targeted drug delivery system that is based on DNA-hybrid-capped mesoporous silica-coated quantum dots (MSQDs); drug release is controlled by

[*] P. Zhang,[+] F. Cheng,[+] Dr. J. Cao, Dr. J. Li, Dr. Q. Min, Prof. Dr. J.-J. Zhu
State Key Laboratory of Analytical Chemistry for Life Science
School of Chemistry and Chemical Engineering
Nanjing University
Nanjing 210093 (P.R. China)
E-mail: minqianhao@nju.edu.cn
jjzhu@nju.edu.cn
R. Zhou
Institute of Life Science, Nanjing University
Nanjing 210093 (P.R. China)
Prof. Dr. C. Burda
Case Western Reserve University, Chemistry Department
10900 Euclid Ave., Cleveland, OH, 44106 (USA)
[+] These authors contributed equally to this work.

[**] This research was supported by the National Basic Research Program of China (2011CB933502) and the National Natural Science Foundation of China (21020102038, 21335004, 21205060, and 21121091). Dr. J. Li also thanks the State Key Laboratory of Analytical Chemistry for Life Science for support (SKLACLS1203).
Supporting information for this article is available on the WWW under http://dx.doi.org/10.1002/anie.201308920.

miRNA. The DNA hybrid was synthesized by coupling anti-miR-21 at the 3′ end of the AS1411 aptamer, which is a guanine-rich oligonucleotide that can form a stable G-quadruplex structure to specifically target nucleolin, which is overexpressed on tumor cell surfaces.[10,17] Multifunctional MSQDs were loaded with Doxorubicin (Dox) and then capped with the DNA hybrid by forming 12 base pairs between parts of anti-miR-21 and the anchor-DNA on the nanoparticles to form a DNA gate to prevent leaking of Dox (Scheme 1). By recognition of AS1411, the nanocarriers

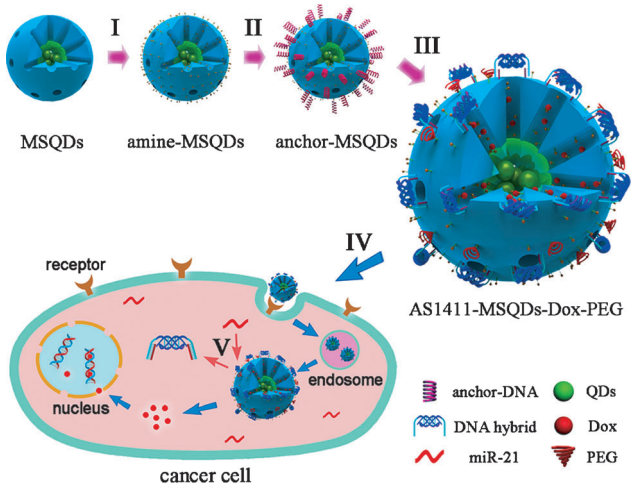

Scheme 1. Preparation and application of miRNA-responsive controlled drug delivery nanocarriers. Stage I: functionalization of MSQDs with amine groups; stage II: conjugation of anchor-DNA; stage III: Dox loading, DNA hybrid capping by forming 12 base pairs with anchor-DNA, and PEGylation; stage IV: AS1411-targeted recognition and endocytosis; stage V: controlled release of Dox by uncapping the DNA hybrid with miR-21 by competitive formation of 22 base pairs.

exclusively entered the target tumor cells, whereas their nonspecific uptake by normal cells was minimized owing to polyethylene glycol (PEG). Subsequently, miR-21, which is overexpressed in the cytoplasm of tumor cells, served as an exclusive key to unlock the gate by competing against anchor-DNA to fully hybridize with anti-miR-21, thereby triggering on-command release of Dox from AS1411-MSQDs-Dox-PEG. At the same time, anti-miR-21 consumed miR-21 strands by complementary base pairing, and thus acted as an inhibitor to suppress the expression of miR-21, which led to an enhanced efficacy of the chemotherapy. Therefore, maximum therapeutic efficacy and minimum side effects were achieved by virtue of the aptamer-targeted delivery and miRNA-targeted drug release.

Transmission electron microscopy (TEM) revealed that all three different types of nanoparticles were of a similar and uniform size with a mean diameter of 100 nm (Figure 1a). However, the hydrodynamic diameter of anchor-MSQDs significantly increased from 105 ± 7 nm to 136 ± 11 nm, which indicates a successful conjugation of anchor-DNA (Supporting Information, Figure S1). Detailed characterization studies (Figure S2 and S3) revealed that the MSQDs possessed well-ordered porous structures with typical MCM-41 hexagonal

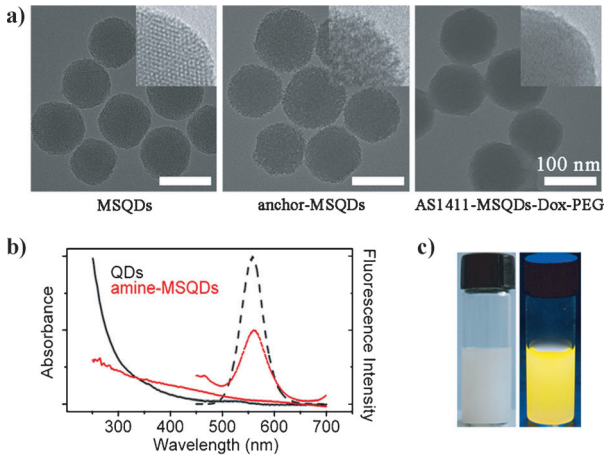

Figure 1. a) TEM images of MSQDs, anchor-MSQDs, and AS1411-MSQDs-Dox-PEG. b) UV/Vis and fluorescence spectra of QDs and amine-MSQDs. c) Photographs of amine-MSQDs with or without UV excitation.

arrangements, high specific surface areas ($787\ m^2\,g^{-1}$), and well-defined pore sizes (ca. 3.8 nm). Furthermore, the success of the surface functionalization processes was confirmed by solid-state NMR spectroscopy (Figure S4) and Fourier transform infrared (FTIR) spectroscopy (Figure S5).[10,18] Meanwhile, by monitoring the variations in the UV/Vis absorbance spectrum, the amount of anchor-DNA that is linked to the anchor-MSQDs could be optimized to be $11.6\ nmol\,mg^{-1}$ (Figure S6). After Dox loading and DNA hybrid capping, AS1411-MSQDs-Dox nanocarriers with a Dox loading capacity of $113.2\ mg\,g^{-1}$ and a DNA hybrid capping amount of $4.6\ nmol\,mg^{-1}$ were obtained (Figure S7). Finally, mPEG-SPA (SPA = succinyl propionate), which can rapidly react with amine residues in an aqueous solution, was conjugated onto the nanocarriers to generate AS1411-MSQDs-Dox-PEG nanoparticles, which exhibited an improved long-term stability in cell culture medium (Figure S8). Moreover, amine-MSQDs displayed strong fluorescence with a quantum yield of 17.1% (Figure 1b,c; see also Figure S9) and remarkable photostability owing to the protection of the silica shell; these properties facilitate the tracking of the intracellular drug delivery.

The mechanism of the miR-21 triggered release was first checked by polyacrylamide gel electrophoresis. The single emission band (lane 1; Figure 2a,b) was assigned to the robust formation of 12 base pairs between anchor-DNA and DNA hybrid. With the subsequent addition of equivalent miR-21 (lane 2), a slower migration rate was observed, which is due to the competitive formation of 22 base pairs between miR-21 and the DNA hybrid, whereas an insufficient amount of miR-21 led to scattering bands (lane 3). Moreover, the addition of nontarget miRNA' only displayed a negligible influence on the displacement binding results (lanes 4,5). Afterwards, the controlled release of Dox from AS1411-MSQDs-Dox-PEG was monitored by measuring its fluorescence at 580 nm. A further Dox leaking of 1.3% was observed from the nanocarriers after the addition of nontarget miRNAs (Figure 2c; step i), which indicates that the designed

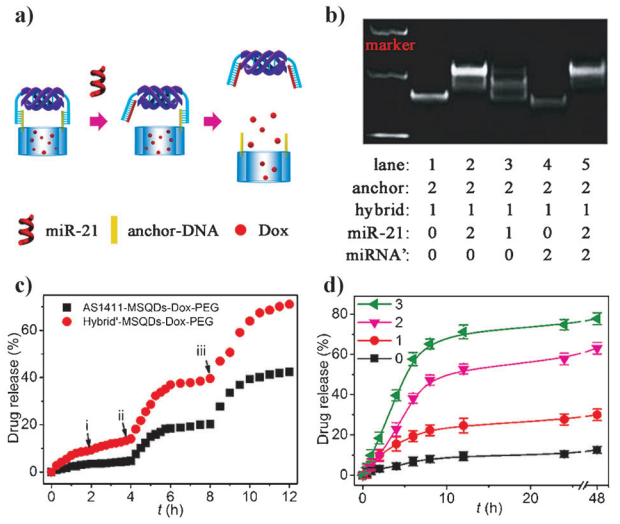

Figure 2. a) Uncapping mechanism by competitive hybridization between miR-21 and DNA hybrid/anchor-DNA. b) Results from displacement binding of miR-21 with DNA hybrid/anchor-DNA by polyacrylamide gel electrophoresis. miRNA' served as the non-target control. c) Release profiles of AS1411-MSQDs-Dox-PEG and Hybrid'-MSQDs-Dox-PEG (single DNA strand as capping domain) after successive addition of non-target miRNA (i), and miR-21 (ii and iii) in phosphate-buffered saline (PBS; 10 mM, pH 5.0). d) Release profiles of AS1411-MSQDs-Dox-PEG with addition of different concentrations of miR-21 in PBS. The ratios of the amounts of added miR-21 to DNA hybrid were 0, 1, 2, 3, respectively.

method is highly selective. However, once the miR-21 molecules were added, rapid release of Dox (15.5% in step ii, 22.1% in step iii) was observed, which is due to the dissociation of the DNA hybrid from the nanocarriers by competitive displacement reactions. In comparison, the use of a control structure of Hybrid'-MSQDs-Dox-PEG with a single DNA strand as the capping domain led to a sustained Dox release in the absence of miR-21, which confirms the importance of the G-quadruplex structure in capping the mesopore channels. The diameter of the G-quadruplex was reported to be 2.4 nm,[10] which is suitable for capping the 3.8 nm wide pore. Furthermore, by adjusting the concentration of miR-21, the release rate and the amount of Dox could be controlled (Figure 2d; see also Figure S10). Considering the possible degradation of the DNA gate, which can be induced by variations in the intracellular pH value and by enzymes, the stability of the drug delivery system was evaluated by determining the release of the drug in different buffer and enzyme solutions (Figure S11). In the absence of miR-21, the DNA hybrid effectively prevented the release of Dox from the nanocarriers even in an acidic environment (pH 5) and in enzyme solution (containing DNase Iendonuclease and a single-stranded DNA binding protein). Upon the addition of miR-21, rapid drug release was observed in all media. Therefore, after conjugation onto the nanoparticles, the function of the DNA gate could be preserved in the presence of endogenous enzymes or in an acidic environment during drug delivery.[19]

To assess the target efficiency and specificity of the AS1411-MSQDs-Dox-PEG, confocal laser scanning microscopy (CLSM) and flow cytometry analysis were performed by determining the fluorescence of the loaded Dox. The fluorescence emission was stronger for HeLa cells than for NIH 3T3 cells because the specific interaction between AS1411 and nucleolin, which is overexpressed on the membrane of HeLa cells, led to an enhanced uptake of the nanoparticles (Figure S12). Otherwise, treatment of the HeLa cells with AS1411 molecules to inhibit the binding affinity of nucleolin would drastically decrease the target efficiency of the nanocarriers and thus reduce the fluorescence intensity in the inhibition assay, corroborating that the uptake was mainly induced by the specific interaction between AS1411 and nucleolin. Moreover, because of the additional PEGylation, the nonspecific adsorption of the AS1411-MSQDs-Dox-PEG onto the NIH 3T3 cells was significantly reduced compared with AS1411-MSQDs-Dox (Figure S12b), resulting in an enlarged uptake distinction between the target cells and normal cells, which is beneficial for alleviating side effects.

The traceability of the AS1411-MSQDs-Dox-PEG nanocarriers was investigated by CLSM during intracellular delivery and drug release. Most of the nanocarriers were trapped inside the endosome/lysosome, while some had successfully escaped into the cytoplasm by means of the proton-sponge effect (Figure S13–S15).[20] Upon uncapping by endogenous miR-21, Dox gradually diffused from the nanocarriers into the cell nucleus, whereas the nanoparticles were left outside because of size exclusion, as the nuclear pores have a diameter of only 20–70 nm.[21] Consequently, the interaction between Dox and DNA inhibits macromolecular biosynthesis and induces cell death.[22] The therapeutic efficacy of the nanocarriers was evaluated by MTT tests (MTT = 3-(4,5-dimethylthiazol-2-yl)-2,5-diphenyltetrazolium bromide; Figure S16). By virtue of the efficient capping and specific recognition of the DNA hybrid, a low dosage of the AS1411-MSQDs-Dox-PEG nanocarriers led to a sustained lethality of the HeLa cells; however, damage to NIH 3T3 cells, which could be caused by weak nonspecific adsorption, was very small, which indicates a high therapeutic efficacy and negligible side effects. Nevertheless, although miR-21 is overexpressed in most cancer cells,[16c] its relatively low concentration triggers insufficient uncapping at high concentrations of AS1411-MSQDs-Dox-PEG, which leads to an unsatisfactory mortality rate of the HeLa cells.

To maximize therapeutic efficacy, a greater number of miR-21 strands are needed to uncap the AS1411-MSQDs-Dox-PEG nanocarriers for drug release. To date, many methods have been developed to modulate the expression of miRNAs; these include the delivery of miRNAs or their antisense strands, the use of ionizing radiation, and treatment with molecular inhibitors.[23] As a proof of concept, we modulated the expression levels of miR-21 by transfecting synthesized miR-21 into HeLa cells. Quantitative polymerase chain reaction (qPCR) experiments were conducted to assess the expression levels of intracellular miR-21 after transfection with miR-21 mimics and antisense oligonucleotides, which contribute to up- and down-regulation, respectively (Figure 3c). The expression alteration showed an obvious impact on drug release (Figure 3a and Figure S17), as a burst release of Dox was observed after the first six hours owing to the

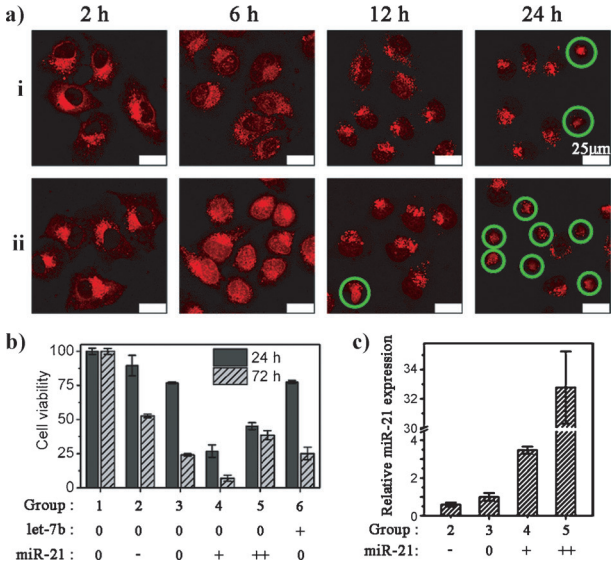

Figure 3. a) CLSM images of HeLa cells without (i) or with (ii) transfection of miR-21 before incubation with AS1411-MSQDs-Dox-PEG. The apoptotic bodies of cells were marked with a circle. b) Cell viability of HeLa cells. Group 1 was used as the control without any treatment. After transfection with miRNA mimics (+) or inhibitors (−), HeLa cells in groups 2–6 were incubated with AS1411-MSQDs-Dox-PEG. let-7b was used as the non-target miRNA in group 6, and had only a minute influence on the cell viability. c) The miR-21 expression levels of HeLa cells, as determined by qPCR after transfection with miRNA mimics (+) or inhibitors (−; same sequence as in Figure 3b).

accelerated uncapping after miR-21 transfection. A mass of apoptotic bodies (marked in the confocal images; Figure 3a and Figure S18) appeared after 24 hours, which indicated that most of the cells were induced to apoptosis, suggesting an intensified cytotoxicity compared with the control group. MTT results further confirmed that the therapeutic efficacy dramatically improved with an increase in the amount of intracellular miR-21 (Figure 3b). However, unexpected high cell viability was observed after introducing too much of miR-21 into the HeLa cells (Group 5), which might be attributed to the fact that an increase in the amount of intracellular free miR-21 strands enhanced the resistance of the cells to Dox by blocking the expression of critical apoptosis-related genes in the HeLa cells.[16b,24] Therefore, the release of Dox from AS1411-MSQDs-Dox-PEG nanocarriers can be controlled on command by adjusting the expression of miR-21. In return, the consumption of miR-21 by hybridizing with the DNA hybrid objectively results in down-regulation of miR-21 and thus activates the caspase-dependent apoptotic cell death pathway, exerting a positive effect on the cancer therapy.

In summary, a DNA hybrid that consists of an aptamer and an antisense oligonucleotide of miR-21 was synthesized as a gatekeeper to cap nanocarriers. Because of the overexpression of nucleolin and miR-21 in cancer cells, aptamer-targeted delivery and miRNA-controlled release were achieved simultaneously, which resulted in maximum therapeutic efficacy and minimal side effects. More importantly, considering the complexity of the regulation network, which is composed of miRNAs and their multiple gene targets, this miRNA-responsive drug delivery model paves the way for combining chemotherapy and gene therapy to obtain an optimized therapeutic efficacy in cancer treatment. Furthermore, with the development of cell-SELEX (SELEX = systematic evolution of ligands by exponential enrichment) and miRNA expression profile technology,[25] more specific aptamers and exclusive miRNAs in pathological cells can be screened and applied to this versatile method to fabricate targeted and personalized drug delivery systems for the clinical treatment of human diseases.

Received: October 13, 2013
Revised: November 21, 2013
Published online: January 27, 2014

Keywords: DNA hybrids · drug delivery · mesoporous materials · microRNA · nanocarriers

[1] Z. Li, J. C. Barnes, A. Bosoy, J. F. Stoddart, J. I. Zink, *Chem. Soc. Rev.* **2012**, *41*, 2590–2605.
[2] a) P. P. Yang, S. L. Gai, J. Lin, *Chem. Soc. Rev.* **2012**, *41*, 3679–3698; b) Y. Wang, J. He, J. W. Chen, L. B. Ren, B. W. Jiang, J. Zhao, *ACS Appl. Mater. Interfaces* **2012**, *4*, 2735–2742.
[3] J. L. Vivero-Escoto, I. I. Slowing, C. W. Wu, V. S. Y. Lin, *J. Am. Chem. Soc.* **2009**, *131*, 3462–3463.
[4] J. Zhang, Z. F. Yuan, Y. Wang, W. H. Chen, G. F. Luo, S. X. Cheng, R. X. Zhuo, X. Z. Zhang, *J. Am. Chem. Soc.* **2013**, *135*, 5068–5073.
[5] T. A. Xia, M. Kovochich, M. Liong, H. Meng, S. Kabehie, S. George, J. I. Zink, A. E. Nel, *ACS Nano* **2009**, *3*, 3273–3286.
[6] a) E. Climent, R. Martínez-Máñez, F. Sancenón, M. D. Marcos, J. Soto, A. Maquieira, P. Amorós, *Angew. Chem.* **2010**, *122*, 7439–7441; *Angew. Chem. Int. Ed.* **2010**, *49*, 7281–7283; b) C. Chen, J. Geng, F. Pu, X. J. Yang, J. S. Ren, X. G. Qu, *Angew. Chem.* **2011**, *123*, 912–916; *Angew. Chem. Int. Ed.* **2011**, *50*, 882–886.
[7] S. Wu, X. Huang, X. Du, *Angew. Chem.* **2013**, *125*, 5690–5694; *Angew. Chem. Int. Ed.* **2013**, *52*, 5580–5584.
[8] H. Kim, S. Kim, C. Park, H. Lee, H. J. Park, C. Kim, *Adv. Mater.* **2010**, *22*, 4280–4283.
[9] F. Muhammad, M. Guo, W. Qi, F. Sun, A. Wang, Y. Guo, G. Zhu, *J. Am. Chem. Soc.* **2011**, *133*, 8778–8781.
[10] X. J. Yang, X. Liu, Z. Liu, F. Pu, J. S. Ren, X. G. Qu, *Adv. Mater.* **2012**, *24*, 2890–2895.
[11] a) A. Popat, B. P. Ross, J. Liu, S. Jambhrunkar, F. Kleitz, S. Z. Qiao, *Angew. Chem.* **2012**, *124*, 12654–12657; *Angew. Chem. Int. Ed.* **2012**, *51*, 12486–12489; b) Z. Zhang, D. Balogh, F. Wang, I. Willner, *J. Am. Chem. Soc.* **2013**, *135*, 1934–1940.
[12] C. Chen, L. Zhou, J. Geng, J. Ren, X. Qu, *Small* **2013**, *9*, 2793–2800.
[13] F. Q. Tang, L. L. Li, D. Chen, *Adv. Mater.* **2012**, *24*, 1504–1534.
[14] R. Kuner, J. C. Brase, H. Sueltmann, D. Wuttig, *Methods* **2013**, *59*, 132–137.
[15] a) J. Lu, G. Getz, E. A. Miska, E. Alvarez-Saavedra, J. Lamb, D. Peck, A. Sweet-Cordero, B. L. Ebert, R. H. Mak, A. A. Ferrando, J. R. Downing, T. Jacks, H. R. Horvitz, T. R. Golub, *Nature* **2005**, *435*, 834–838; b) L. F. Sempere, M. Christensen, A. Silahtaroglu, M. Bak, C. V. Heath, G. Schwartz, W. Wells, S. Kauppinen, C. N. Cole, *Cancer Res.* **2007**, *67*, 11612–11620.
[16] a) M. D. Jansson, A. H. Lund, *Mol. Oncol.* **2012**, *6*, 590–610; b) Z. X. Wang, B. B. Lu, H. Wang, Z. X. Cheng, Y. M. Yin, *Arch. Med. Res.* **2011**, *42*, 281–290; c) Z. L. Liu, H. Wang, J. Liu, Z. X. Wang, *Mol. Cell. Biochem.* **2013**, *372*, 35–45; d) T. Papagiannakopoulos, A. Shapiro, K. S. Kosik, *Cancer Res.* **2008**, *68*, 8164–8172.

[17] S. Soundararajan, L. Wang, V. Sridharan, W. Chen, N. Courtenay-Luck, D. Jones, E. K. Spicer, D. J. Fernandes, *Mol. Pharmacol.* **2009**, *76*, 984 – 991.
[18] Y. Chen, H. Chen, S. Zhang, F. Chen, L. Zhang, J. Zhang, M. Zhu, H. Wu, L. Guo, J. Feng, J. Shi, *Adv. Funct. Mater.* **2011**, *21*, 270 – 278.
[19] R. Qian, L. Ding, H. Ju, *J. Am. Chem. Soc.* **2013**, *135*, 13282 – 13285.
[20] Y. B. Lim, S. M. Kim, Y. Lee, W. K. Lee, T. G. Yang, M. j. Lee, H. Suh, J. S. Park, *J. Am. Chem. Soc.* **2001**, *123*, 2460 – 2461.
[21] L. M. Pan, Q. J. He, J. N. Liu, Y. Chen, M. Ma, L. L. Zhang, J. L. Shi, *J. Am. Chem. Soc.* **2012**, *134*, 5722 – 5725.
[22] F. A. Fornari, J. K. Randolph, J. C. Yalowich, M. K. Ritke, D. A. Gewirtz, *Mol. Pharmacol.* **1994**, *45*, 649 – 656.
[23] L. Zhao, X. Lu, Y. Cao, *Cell. Signalling* **2013**, *25*, 1625 – 1634.
[24] J. A. Chan, A. M. Krichevsky, K. S. Kosik, *Cancer Res.* **2005**, *65*, 6029 – 6033.
[25] a) Y. Xu, J. A. Phillips, J. Yan, Q. Li, Z. H. Fan, W. Tan, *Anal. Chem.* **2009**, *81*, 7436 – 7442; b) M. Boeri, C. Verri, D. Conte, L. Roz, P. Modena, F. Facchinetti, E. Calabrò, C. M. Croce, U. Pastorino, G. Sozzi, *Proc. Natl. Acad. Sci. USA* **2011**, *108*, 3713 – 3718.

